European Association for the Development of Renewable Energies, Environment and Power Quality (EA4EPQ)

International Conference on Renewable Energies and Power Quality (ICREPQ'10)
Granada (Spain), 23rd to 25th March, 2010

A Study of the Current Disturbance Caused by Wind Induced Vibrations of Photovoltaic Modules

J. Schmid[1], E. Kancsar[1], M. Drapalik[1], V. Schlosser[1], G. Klinger[2]

[1] University of Vienna, Department of Electronic Properties of Materials, Faculty of Physics, A-1090 Vienna, Strudlhofgasse 4, Austria.
Phone number:+43 4277 51428, e-mail: **viktor.schlosser@univie.ac.at**

[2] University of Vienna, Department of Meteorology and Geophysics, A-1090 Vienna, Austria.
e-mail: **gerhard.klinger@univie.ac.at**

Abstract. Mechanical vibrations of a solar module mounting rack cause oscillations in the orientation of the module towards the sun. The resulting intensity oscillations of the incident light originate an a.c. current at the module's terminals.
We have investigated this effect in the laboratory by means of a vibration table and outdoors where wind forces induce vibrations to the mounting rack. Although the collected results are specific and restricted to our experimental set up and environmental situation we deduce that vibration induced current transients and oscillations of a solar module's output most often will be the dominant origin of distortion in the low frequency regime.

Key words

Low frequency disturbance, Vibrations, Photovoltaic power generator.

1. Introduction

The fast increasing capacity of distributed energy resources connected to the grid has recently invoked numerous investigations about the proper interfacing such preserving power quality and avoiding electromagnetic interference [1, 2]. Only little research has been done so far in the study of distortion caused by the power generator itself which is transmitted to the subsequent electric conditioning system [3]. Beside the intrinsic noise of the photovoltaic cells numerous external sources can introduce current transients, spikes and oscillations as illustrated by fig.1.

These noise sources cover a wide frequency range from below 1 Hz typical for cloud movements up to 10 GHz which is caused by satellite communication channels. Although the externally introduced current noise at the terminals of a single module may not exceed several mA in amplitude electrical interconnections of an assembly of modules summarises the noise amplitudes which are conducted to the power conditioning unit.

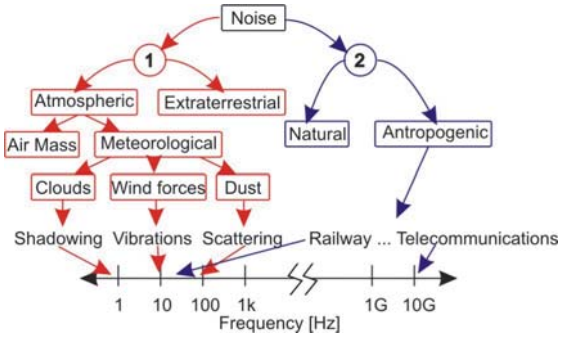

Fig. 1: Origin of externally introduced noise in photovoltaic solar cells, examples and typical frequency ranges: Light fluctuations (1) are branched red, radio frequency emissions (2) are highlighted in blue.

Current transients in the low to very low frequency regime are extremely hard to remove in the circuitry by a low pass filter without the reduction of the useful d.c. output. Because of the need to optimise the exposure of solar modules to the incident sun light they are placed on mounting constructions which easily are stimulated to vibrate. These vibrations cause changes of the module's surface orientation with respect to the incident sun rays. As a consequence light intensity oscillations cause current oscillations. Usually the resonance frequency of a mounting construction for photovoltaic applications is in the low to very low frequency range. As previously reported noise amplitudes below 100 Hz sometimes became the major contribution to the observed noise spectra and were attributed to wind induced vibrations of our test module [4].

Currently we investigate the effect of vibration induced current oscillations in detail in the laboratory and under outdoor conditions. In this contribution we present some exemplary results from our measurements in order to illustrate the importance of mechanical vibrations as a major source of distortion.

In the laboratory we examined the effect of changing light intensity distribution caused by the vibrations relative to the incident light beam over the area of the solar cells, with respect to different loads and circuit arrange-

ments (i.e. parallel, serial and single). Thus we were able to derive some basic characteristics of the behaviour of ultra low frequency distortion in solar modules.

To supplement and confirm our results a simulation with the circuit simulation program Qucs [5] has been undertaken.

2. Experimental Indoor

In order to conduct the measurements a vibration table has been constructed. The solar cell is exposed to some mechanical strain and a roughly sinusoidal change of the incoming light flux. This set up tries to emulate the real ambient conditions of a solar cell with respect to vibrational disturbances as accurately as possible, while still being reproducible.

It basically consists of a subwoofer that has been mounted on a self constructed aluminium rack. The subwoofer's membrane was coupled to a plexiglass plate forming the vibration table. The vertical Z-axis of the vibration table was displaced by a sinusoidal excitation of the subwoofer at different frequencies

Onto the plexiglass plate a holder is fixed where solar cells can be easily attached and removed by a hook and loop fastener. The device allows to change the angle of misorientation determined by the cell's surface vector and the optical axis of the light source within a horizontal plane. This angle was later varied to determine the angle dependency of the distortion signal. The solar cells are illuminated by a halogen lamp (12V/20W).

Furthermore a tilted mirror is fixed to the plexiglass. It reflects a laser beam, that first passes an aperture, towards a linear sensor array (TAOS TSL 1401). The array consists of 128 photodiodes. Thus we are able to measure the deflection of the vibration table with an accuracy of 250 µm.

To test the different solar panels under various load conditions a circuit has been designed. It consists mainly of 8 resistors interconnected through 8 relays which can be switched on and off individually through the digital ports of a NI-6009 IO interface. Hence 256 different configurations of the resistors are possible ranging up to 937 Ω in steps of about 7 Ω.

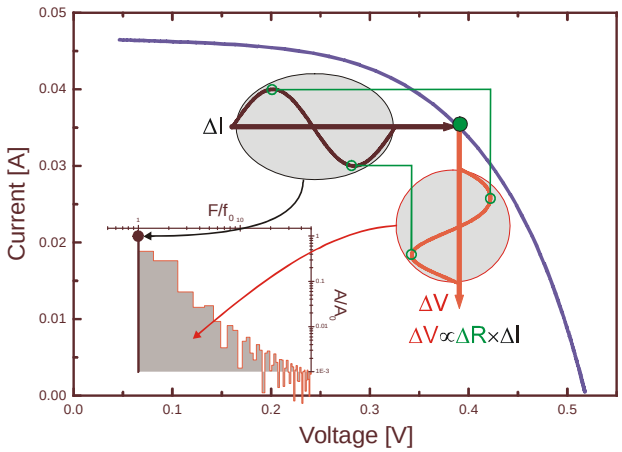

Fig. 2: Transfer function between modulated current and resulting voltage signal. In the lower left corner a power spectrum, derived from a circuit simulation illustrates the problem.

In the experimental set-up the voltage of the solar cells at different loads is measured. Even if the excitation frequency is very well defined the resulting a.c. output will most likely be distorted. This can be explained by the fact that the power yield not only depends on the incoming light flux but on the operating condition as well ($P_{inc}(I(R),V(R))$.

In the equivalent circuit diagram only the current was modulated. The dependence of the current modulation and the resulting voltage modulation is described through a transfer function as can be seen in Fig. 2. Especially in the areas of strong non linearity the excited signal will undergo a strong distortion

To take this effect into account transient disturbances of the solar cell output have been measured in two different ways. To get the whole spectrum of the output a low noise preamplifier was connected to the solar cell. The signal of the low noise preamplifier was then recorded via the NI USB 6251 data acquisition interface and analysed with NI LabView program. A fast Fourier transformation was applied. An exemplary visualisation is shown in Fig.3 for a mechanical excitation at 8 Hz.

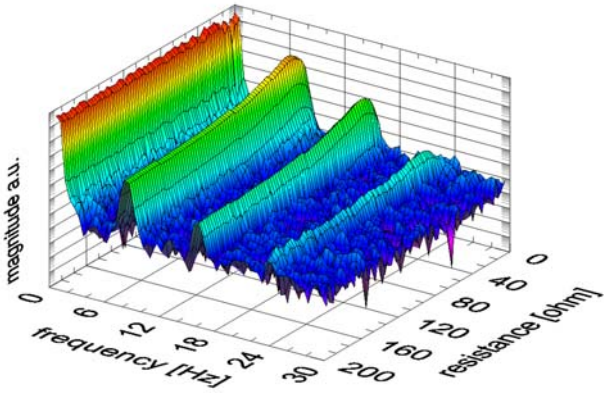

Fig. 3. Fast Fourier transformed frequency spectrum for variable loads. The base frequency and two harmonics can be seen quite well.

For each resistor the flattened resonance frequency and its harmonics were summed up. Thus gaining an amplitude for the overall distortion, specifically caused by the vibrational effect.

Alternatively a lock-in amplifier was connected to the solar cell, giving the V_{rms} of the fundamental frequency only.

These measurements where undertaken with two small multicrystalline solar cells. They were operated singularly, series connected and parallel connected. Not changing anything about the experimental set-up, lest the wiring.

Additionally current-voltage characteristics of the solar cells have been recorded to determine operating point conditions. The results can be seen in Table I.

	Cell #1	Cell #2
Power [mW]	5.9	7.7
Resistance [Ω]	25.92	16.5

Table I. – Key data of operating point conditions

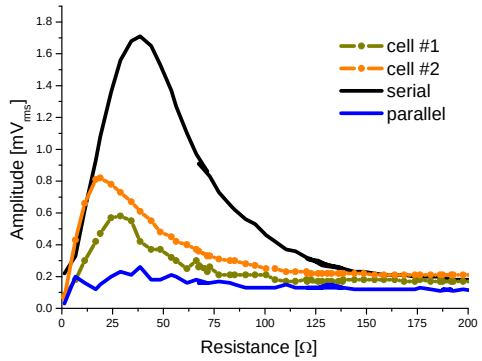

Fig. 3. Amplitude of transient a.c. signal, derived from a lock-in amplifier. Measurement was done at 8 Hz excitation frequency.

Fig. 3 shows the results of the measurement. The maximum of the resonance amplitude appears close to the operating point, maybe somewhat shifted to lower resistance values as the simulation suggests. The two cells connected in series yield a signal which at its peak is greater than the sum of the two single cells at their operating point. This effect even is slightly intensified when looking at the results of the measurement taken with the preamplifier. In both experimental set-ups the parallely connected cells barely seem to be affected by the disturbances at all.

3. Simulation of the a.c. Behaviour of the Solar Cells

Based on the measured current-voltage curve of two c-Si solar cells a simulation in qucs [5] was done. To simulate the change of the incoming light flux the constant photo current was superimposed with a sinusoidaly alternating current. A schematic circuit diagram of the simulation is shown in Fig. 4.The main parameters of the simulation are shown in table II.

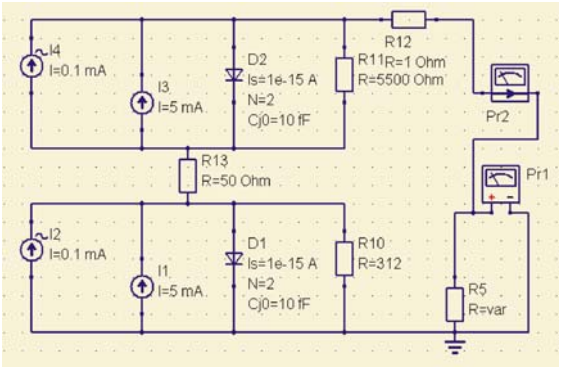

Fig. 4. Screenshot of the qucs-circuit simulator. Series connected.

In Fig. 5 the result of the simulation of a series circuit (left hand diagram) and a parallel circuit (right hand diagram) are juxtaposed. Both simulations were executed with identical parameters. Characteristic current voltage curves (i.e. the black line, scaled according to the left hand side y-axis) and the power curve (i.e. the blue line, scaled according to the left hand side y-axis) were derived from the direct current simulation. The $I(V)_{DC}$ curve was used to differentiate $\Delta V/\Delta R_{load}$. The result was multiplied with R_{load} and is represented as orange line with the corresponding right hand side y-axis scaling. The transient simulation was carried out for a time interval of 200ms (two periods for f=10Hz) yielding 11 pairs of variates of averages of V_{mean} and I_{mean} which are plotted as symbols (black circles) over the characteristic curves. The a.c. component of the signalwas Fourier-transformed and evaluated according to the amplitude of the base frequency. (i.e. the red symbols, scaled according to the right hand side y-axis). For both simulations the a.c.-amplitudes accord sufficiently well with the differentiation of the characteristic curve of the direct current simulation which suggests that only minor signal-distortion takes place. However it can be seen that the maximum of the a.c.-signal lies a little below the maximum power point of the characteristic I(V) curve in relation to the voltage.

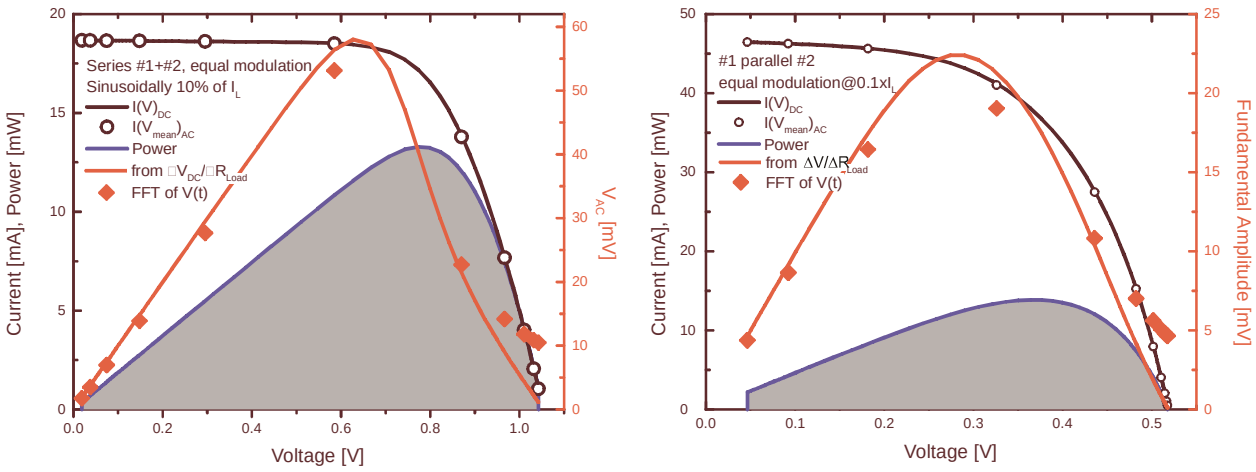

Fig 5: Results of the simulation for a series connection (left) and a parallel connection (right) of the two cells.

Parameter	Cell #1	Cell #2
Diode factor n	2	2
Saturation current I_0	0.93µA	0.655µA
Series resistance R_S	0.303Ω	5.09Ω
Shunt R_{SH}	5.55kΩ	0.312kΩ
Photo current I_L	18.6mA	28.5mA
Load Resistance R_{load}	1Ω-1kΩ	1Ω-1kΩ

Table II. – Main parameters of simulation

4. Experimental outdoor

The outdoor investigations were done in central Vienna at the roof top of the institute building: Latitude = 48.22165 N, longitude = 16.3558 E and altitude = 202 m determined by GPS. As rack a two axis gimbal mount originally designed for solar irradiance measurements was used which allowed us to vary the inclination manually with a simple lever lock. The orientation from North, Ψ_0 was kept constant at 180.7 deg in our experiments. A 10 W_p flat solar module of multycrystalline silicon cells together with an encapsulated three axis geophone from Mark Products Inc. was mounted on the rack. The panel is specified for 17 V operation with an output current of 0.6 A which would require a 28 Ω load impedance. We operated the module either with a 21 Ω/25W resistor monitoring the photo-current which remains close to short circuit current conditions at all intensity levels. Alternatively the module was connected to an Agilent Technologies 50V/3A power supply module (N6762A) inserted in a N6705A frame with integrated measurement capabilities for voltages and currents up to 10 kHz. The power supply was capable to serve as adjustable sink and allowed us to carry out measurements at different operating points. The specifications of the three geophones are identical and as follows: Sensitivity is2 6.9V×$(m/s)^{-1}$, frequency limit is 4.5 Hz, attenuation for lower frequencies is 24dB/oct. Beside this core parameters the following ambient parameters were locally recorded during the measurements: incident intensity by means of a Kipp & Zonen pyranometer type CM6B, temperature and the wind speed in the range between 1.5 m/s and 15 m/s by an anemometer from Wilh. Lambrecht.

Horizontal and vertical geophone velocities were recorded simultaneously with the light generated current at sample rates of at least 1 kSs^{-1}. The velocities were converted to displacement co-ordinates, Δx, Δy and Δz by numerical integration. In order to examine the variation of the panel's orientation towards the sun and thus the intensity variations of the incident sun light on the module's surface a transformation in rotation angles in analogy to the yaw-pitch-roll model used in Aeronautics is favourable [6]. The three angles defined by the model are Ψ, Θ and φ where Ψ is the horizontal angle from North and is identical to the definition of Ψ_0 above. The pitch angle Θ is the inclination from the horizon and may not be confused with the definition of the tilt angle commonly used in photovoltaic terminology which is defined by the angle between the horizontal plane and the module's plane. The pitch angle Θ equals the angle between the surface vector and the horizontal plane. The tilt angle therefore relates to the pitch angle by (90-Θ) deg. The roll angle φ describes a rotation coplanar to the module. Therefore at least for flat plate modules φ should not contribute to intensity variations caused by the module's displacement. During our experiments we varied the inclination Θ_0 between 90 deg (tilt angle=0 deg, horizontal module position) and 5 deg (tilt angle=85 deg, steep module position). The transformation is given by the following equations:

$$[x+\Delta x, y+\Delta y, z+\Delta z] = [x, y, z] R_\Psi R_\Theta R_\varphi \quad (1)$$

$$R_\Psi = \begin{bmatrix} \cos\Psi & \sin\Psi & 0 \\ -\sin\Psi & \cos\Psi & 0 \\ 0 & 0 & 1 \end{bmatrix} \quad (2)$$

$$R_\Theta = \begin{bmatrix} 0 & 0 & 1 \\ \cos\Theta & \sin\Theta & 0 \\ -\sin\Theta & \cos\Theta & 0 \end{bmatrix} \quad (3)$$

$$R_\varphi = \begin{bmatrix} \cos\varphi & \sin\varphi & 0 \\ -\sin\varphi & \cos\varphi & 0 \\ 0 & 0 & 1 \end{bmatrix} \quad (4)$$

Assuming the mounting rack to be a rigid body, solely the horizontal displacement given by Δx and Δy is independent whereas the vertical component Δz is a function of Δx and Δy. Consequently calculating the variation in orientation ($\Delta\Psi$) and inclination ($\Delta\Theta$) further simplifies..

5. Results and discussion

Prior to evaluating data at different weather conditions mechanical vibrations were introduced by applying short manual forces to the mounting rack. This was done by simply pushing or pulling the rack on a clear sunny day during periods where the wind velocity was below detection limits. Knowing the horizontal displacement and the sun's position the effect of varying misorientation of the module's surface relative to the geometrical path of sun rays and thus the variation of the incident light intensity, P_{inc} on the module's surface were calculated as well as the vertical displacement for the rigid body simplification. A comparison between the measured and calculated values of Δz shows that the experimentally observed elongation always was at least one order of magnitude larger than calculation. That indicates that the rigid body assumption is not justified. None the less a comparison of the model calculations of oscillating P_{inc} and the recorded module's current I_{module} qualitatively agree fairly well in several cases. After the application of a short force in North – South direction the rack is horizontally displaced at similar amplitudes as well in N-S as in E-W direction. The magnitude was generally less than 2 mm in one direction. The rack oscillates at frequencies between 4 Hz and 5 Hz. The frequency shifts with the centre of mass of the system which depends on the adjusted inclination since the construction is not well balanced in the centre of the gimbal axis. The frequency of the E-W displacement always differed somewhat from the frequency of the N-S displacement resulting in a rather complex hori-

zontal trace of the total displacement. The observed damping time constant typically was about 4 s. Vertical displacement oscillations occurred at much higher frequencies of 16 Hz to 18 Hz. In order to extract the measured photo-current oscillations in time intervals of 2 s in a first step a linear fit accounting for the current d.c. value of the photo-current, I_{DC}, and potentially present slow variations of sun light intensity was performed. The residual of the photo-current, I_{AC}, was Fourier Transformed and the amplitude spectra were compared with the displacement oscillations. Within the uncertainties due to changing ambient conditions during the various experiments the magnitude of the a.c. photo-current increases linearly with the amplitude of horizontal displacement. At different incident light intensities the relative a.c. photo-current defined as the ratio $I_{rel}=I_{AC}/I_{DC}$ remains almost constant for similar excitation conditions of the mounting rack.

Model calculations of the variation of the incident light intensity P_{inc} were carried out using the measured horizontal displacement amplitudes and compared with the relative changes in the module's photo-current. Beside the simplifications of the model described above it shall be noted that the calculation accounts solely for direct radiation with a geometrical light pass.

Since for our load resistor $I_{module} \approx I_{sc} \propto P_{inc}$ is valid in all cases the relative amplitudes of as defined below are compared:

$$P_{rel} = \frac{P(\Psi_0 + \Delta\Psi(t), \Theta_0 + \Delta\Theta(t)) - P(\Psi_0, \Theta_0)}{P(\Psi_0, \Theta_0)} \quad (5)$$

$$\Delta\Psi(t) = f(\Delta x(t), \Delta y(t)) \quad (6)$$

$$\Delta\Theta(t) = g(\Delta x(t), \Delta y(t)) \quad (7)$$

Ψ_0 and Θ_0 are the static, undisturbed angles of the module's orientation. The functions f and g are the inverse operations to Eq. 1.

Subsequent measurements with different module inclination were carried out using manual forces in N-S direction and measured and calculated magnitudes of the oscillations were compared (fig.6). The measurements were done in the afternoon the 20th August at about 16:30 in the afternoon where the misorientation of the module to the incident sun rays was between 30 deg and 75 deg depending on the inclination shown in fig.6 as magenta coloured line (right axis). The smallest deviation in the module's orientation would be for a tilt angle of 17 deg.

For Θ_0<45 deg calculations (orange coloured line in fig.6) and experimentally observed current oscillations (symbols) are in fair agreement. However calculations result in significantly to high values at low misorientation angles most likely due to the unjustified assumption of a rigid body construction. Although the relation between misorientation angle and the magnitude of distortion can be clearly seen by comparing the tendency of the symbols with the magenta line in fig.6 obviously it is not a simple linear dependence. A little surprising is the circumstance that the smallest current amplitudes do not occur at minimal misorientation. The minimum in the first case was experimentally observed at an inclination angle of 60 deg, whereas the least misorientation would be around 70 deg of inclination. For larger misorientation the distortion increases stronger than linear.

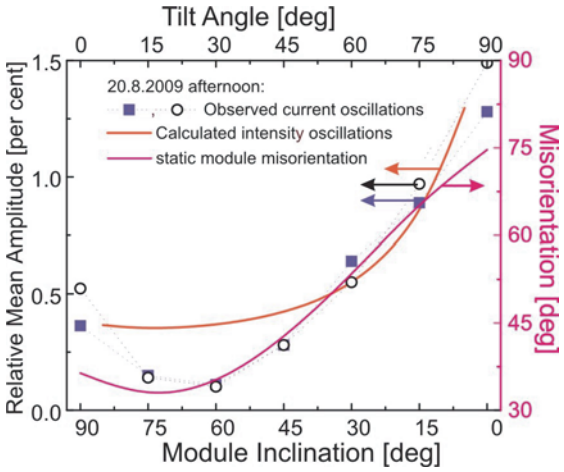

Fig. 6: Dependence of the magnitude of vibration induced current oscillations on the module's inclination

On several days with different weather conditions as by means of wind speed and cloud cover current oscillations, vibrations and wind velocities were monitored during the day at sampling rates of 10 kSs^{-1}. In the period of observation the highest recorded wind speeds were a little more than 15 ms^{-1}. The cloud cover ranges from dense rain clouds to clear blue sky. On average the observed displacement amplitudes and corresponding photo-current oscillations with respect to the panel orientation towards the sun scale directly with the average wind speed. Since we assume that vibrations are preferentially introduced by a sudden change in wind speed we tried to correlate the acceleration obtained from the wind speed recordings with the appearance of high displacement and photo-current oscillations. The response time of our anemometer was determined to be 0.75 s which seems to be sufficiently fast enough to obtain acceleration in real time. However only in a few out of many examined cases we could resolve a doubtless coincidence between wind acceleration and rack vibrations. One major reason presumably is the distance between the location of the rack and the position of the anemometer of more than 5 m which was necessary due to the limited cable length between anemometer head and electronic unit which is placed in house. Therefore we currently restrict our observations on statistical data evaluation A typical example is given in fig.7 which shows the number of occurrences where the amplitude at a distinct frequency in the monitored frequency range of 2.5 Hz to 5 kHz is the largest. Two results are shown for similar ambient conditions but different inclination angles, 45 deg and 15 deg respectively. In order to ease the comparison the occurrence count was normalised to the total number of samples. Although the wind speeds on average and on peak are low in about 50 per cent of all events the largest amplitude was seen at the typical vibration frequency of 5 Hz. The peaks above 100 Hz were identified to arise from electromagnetic distortion caused by a large cooling unit near by. Although both distributions are similar the magnitude of the largest oscillations differ significantly. For an inclination of 45 deg a peak value of

0.76 mA or 0.13 per cent was recorded. During the observation with an inclination of 15 deg where the module was mounted steeper than before the largest current amplitude was 6.29 mA or 1.37 per cent which is in agreement with our experiments on the inclination dependency of the vibration effect.

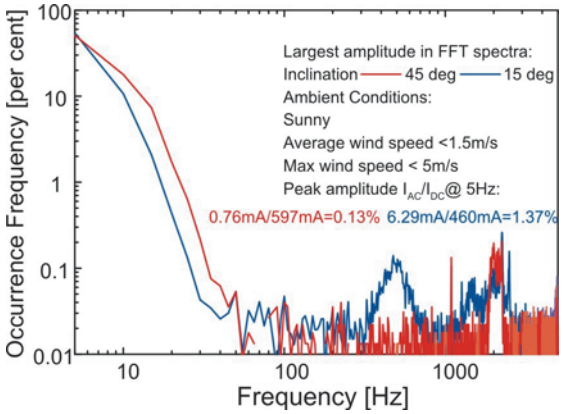

Fig. 7: Example of statistical evaluation showing the relative number of occurrences that the largest amplitude was observed at a certain frequency.

6. Conclusion

Although the presented exemplary results were obtained on an individual small photovoltaic system we believe that vibration induced current oscillations caused by wind forces are a widespread and often the dominant source of low frequency distortions. Once several conditions are met at the same time the magnitude of current oscillations easily can exceed one per cent of it's d.c. Value.

The effect of changing light intensity distribution over the area of the solar cells, with respect to different loads and circuit arrangements is yet to be fully understood. However as well in the laboratory experiments as in the simulation it became clear that the ratio of a.c. current to amplitude is significantly higher when the cells are connected in series than when they are connected parallely.

The simulation as well as the differentiated $I(V)_{DC}$ curve suggest that the maximum of the distortion signal lies below the maximum power point of the characteristic I(V) curve in relation to the voltage. This however could not yet be confirmed or falsified by the experimental measurements conducted.

In the outdoor observations the magnitude of oscillations depend on the mounting construction and will increase with increasing wind forces. Due to thermal management of photovoltaic collectors construction design favours good ventilation conditions which in return eases wind attacks. Thus vibration induced distortion appears to be unavoidable.

Low incident angles of direct sun radiation can reduce the magnitude of the distortion. Therefore tracked concentrating systems potentially will experience less distortion than building integrated photovoltaic facades. Although in the first case the mounting system permits large displacements caused by external forces it is permanently facing the sun. Due to their large inclination angles facades are considerably misoriented towards the sun most of their operation time.

Acknowledgement

The support by Christian Bauer from the sales representative of Agilent Technologies in Austria is highly acknowledged.

References

[1] Bollen, M., Yang, Y., Hassan, F., Proc. of the ICHQP XIII, IEEE, 2008, 8.

[2] Chicco, G., Schlabbach, J., Spertino, F.,Solar Energy, 2009, **83**, 10226.

[3] Di Piazza, M. C., Serporta, C., Tinè, G., Vitale, G., Proc. of IEEE International Conference on Industrial Technology, 2004, **2**, 672.

[4] Drapalik, M., Schlosser, V., Schmid, J., Bajons, P., Klinger, G., Proc. 23rd ECPVSEC Conference, 2008, 3367.

[5] Quite universal circuit simulator at http://qucs.sourceforge.net/index.html

[6] http://en.wikipedia.org/wiki/Yaw_pitch_and_roll